Molecular Biology of the Cell
Vol. 8, 455–467, March 1997

PF20 Gene Product Contains WD Repeats and Localizes to the Intermicrotubule Bridges in *Chlamydomonas* Flagella

Elizabeth F. Smith and Paul A. Lefebvre*

Department of Genetics and Cell Biology, University of Minnesota, St. Paul, Minnesota 55108

Submitted October 9, 1996; Accepted December 26, 1996
Monitoring Editor: J. Richard McIntosh

The central pair of microtubules and their associated structures play a significant role in regulating flagellar motility. To begin a molecular analysis of these components, we generated central apparatus-defective mutants in *Chlamydomonas reinhardtii* using insertional mutagenesis. One paralyzed mutant recovered in our screen contains an allele of a previously identified mutation, *pf20*. Mutant cells have paralyzed flagella, and the entire central apparatus is missing in isolated axonemes. We have cloned the wild-type *PF20* gene and confirmed its identity by rescuing the *pf20* mutant phenotype upon transformation. Rescued transformants were wild type in motility and in axonemal ultrastructure. A cDNA clone containing a single, long open reading frame was obtained and sequenced. Database searches using the predicted 606-amino acid sequence of *PF20* indicate that the protein contains five contiguous WD repeats. These repeats are found in a number of proteins with diverse cellular functions including β-transducin and dynein intermediate chains. An antibody was raised against a fusion protein expressed from the cloned cDNA. Immunogold labeling of wild-type axonemes indicates that the PF20 protein is localized along the length of the C2 microtubule on the intermicrotubule bridges connecting the two central microtubules. We suggest that the *PF20* gene product is a new member of the family of WD repeat proteins and is required for central microtubule assembly and/or stability and flagellar motility.

INTRODUCTION

Although the structure and function of the dynein arms in flagellar axonemes have been intensively studied (reviewed in Witman, 1989; Porter, 1996), much less is known about the mechanism by which dynein-induced microtubule sliding is regulated to produce complex flagellar waveforms. One of the most compelling models for axonemal motility suggests that the central pair regulates dynein-mediated microtubule sliding (for reviews, Smith and Sale, 1994; Dutcher, 1995; Porter, 1996). The central pair of microtubules rotates once per beat (Omoto and Kung, 1979; Hosokawa and Miki-Noumura, 1987), allowing a periodic interaction of the central pair projections with the radial spoke heads (Warner and Satir, 1974). A signal is transduced via the radial spokes to the inner and outer dynein arms, possibly through the dynein regulatory complex (Piperno *et al.*, 1992; Smith and Sale, 1992). The nature of this signal is unknown but recent evidence suggests that specific dynein subforms are differentially regulated by a phosphorylation event that is dependent on the radial spokes (Howard *et al.*, 1994).

Understanding how axonemal structures contribute to flagellar motility will require the identification and characterization of the individual protein components of these structures. Substantial progress has been made in the molecular dissection of the inner and outer dynein arms (reviewed in Porter, 1996) and radial spoke components (reviewed in Curry and Rosenbaum, 1993), but analysis of central apparatus components has been limited. Early attempts to identify and characterize central apparatus components combined ultrastructural and biochemical techniques to analyze several *Chlamydomonas* mutants with defects in the

* Corresponding author.

central apparatus. Adams *et al.* (1981) and Dutcher *et al.* (1984) determined that at least 23 polypeptides (in addition to α and β tubulin) comprise the central apparatus. Some of these polypeptides are uniquely associated with either the C1 microtubule or the C2 microtubule, indicating that the two microtubules may be functionally specialized. Further biochemical characterization of these central apparatus components has been challenging but several observations of interest have been reported recently. Miller *et al.* (1990) demonstrated that specialized structures capping the distal ends of the central pair microtubules are recognized by an antibody to a kinetochore antigen, and Bernstein *et al.* (1994), Fox *et al.* (1994), and Johnson *et al.* (1994) demonstrated that kinesin-related proteins are components of the central apparatus.

Some central apparatus components must play a role in the assembly and stability of the central microtubules. The microtubules of the central pair assemble with their plus ends distal to the cell body (Euteneuer and McIntosh, 1981), the same polarity observed for the nine doublet microtubules (Allen and Borisy, 1974; Binder *et al.*, 1975); but unlike the nine doublet microtubules, they are not nucleated from the basal bodies and are capped by specialized structures which prohibit microtubule assembly from their distal ends in vitro (Dentler and Rosenbaum, 1977; Dentler and LeCluyse; 1982). Often, a single mutation in one central apparatus component results in the instability of one central microtubule or the failure of the entire central apparatus to assemble. Therefore, not only is the central apparatus involved in regulating flagellar motility, but some of the central apparatus components may represent microtubule nucleation proteins required for initiation of microtubule assembly.

We have begun a molecular dissection of the central apparatus by generating mutants defective in the central apparatus using an insertional mutagenesis technique in which the gene responsible for the mutant phenotype is tagged and amenable to cloning. The first gene cloned in this effort was *PF16*, which encodes a protein that contains armadillo repeats and localizes to the C1 microtubule (Smith and Lefebvre, 1996). In this report, we describe the cloning of the *PF20* gene and characterize its gene product. The flagella of *pf20* cells are paralyzed and isolated axonemes are predominantly lacking the entire central apparatus. The *PF20* gene encodes a protein of approximately 66 kDa, containing five contiguous G-β or WD repeats (Neer *et al.*, 1994). Immunolocalization experiments using antibodies generated against the PF20 protein expressed in vitro demonstrated that the PF20 protein localizes along the length of the C2 microtubule and is associated with the intermicrotubule bridge connecting the two central microtubules. The localization data and mutant phenotype suggest that the PF20 protein is most likely involved in the assembly and stabilization of the central pair microtubules.

MATERIALS AND METHODS

Cell Strains and Media

Insertional mutants were obtained by transforming strain A54-e18 (*nit*1–1, *ac*17, *sr*1, mt^+) with the plasmid pMN56 containing the *NIT1* gene encoding nitrate reductase (Fernandez *et al.*, 1989). Transformed strains with defective motility phenotypes were backcrossed to strains L5 (*nit*1–305, *apm*1–19, mt^+) and L8 (*nit*1–305, *apm*1–19, mt^-) provided by L.W. Tam (University of Minnesota, St. Paul, MN). The *pf15* strain (CC807) and *pf20* strains (CC22 and CC1030) were provided by the *Chlamydomonas* Genetics Center (Duke University, Durham, NC). Strain CC1030 is strain $pf20.3C^+$ (Adams *et al.*, 1981) and strain CC807 is strain $pf15A^+$ (Witman *et al.*, 1978). The *arg7* strain (Lux and Dutcher, 1991) used to construct double mutants for cotransformation experiments was provided by M. Porter (University of Minnesota). All cells were grown in constant light in SGII, SGII-NO_3 (Sager and Granick, 1953; Harris, 1989; Kindle, 1990; Tam and Lefebvre, 1993) or TAP media (Gorman and Levine, 1965). High-efficiency transformation, mutant selection, and genetic analyses were performed as described in the study by Smith and Lefebvre (1996).

Isolation of Genomic Sequence Flanking the Integrated Plasmid

Genomic DNA flanking the insertion site of the integrating plasmid in the mutant A10 was obtained by constructing a genomic DNA library using the λFIX II vector (Stratagene, La Jolla, CA). Genomic DNA (20 μg) was partially digested with 0.075 U of *Mbo*I/μg of DNA at 37° for 1 h. Following partial fill-in, the DNA was sequentially extracted using phenol, phenol:chloroform (1:1), and chloroform, precipitated in ethanol, and resuspended in TE to a concentration of 0.5 μg/μl. The DNA was ligated to the λFIX II vector arms (Stratagene) and packaged using the Gigapack II XL packaging extract (Stratagene) according to protocols provided by the supplier. The resulting library was transfected into XL1-Blue MRA(P2) host cells (Stratagene) and screened using a labeled fragment from the 5′ end of the *NIT1* gene as a hybridization probe. Phage DNA from positive plaques was prepared from 25-ml cultures by polyethylene glycol precipitation (Chisholm, 1989). Genomic DNA flanking the plasmid insertion site was identified by digesting the DNA from positive λ clones with various enzymes and identifying fragments which did not hybridize with radiolabeled DNA from the plasmid pMN56. Procedures for probe isolation, DNA blot analysis, and plaque-lift hybridizations were described previously (Smith and Lefebvre, 1996).

Cloning PF20: Library Screening and Mutant Rescue

A genomic library constructed with DNA from the wild-type strain 21 gr mt^+ in the λ phage vector λFIXII (Schnell and Lefebvre, 1993) was screened using a fragment of cloned genomic DNA flanking the insertion site in the mutant strain A10 as a probe (Figure 1). A second genomic library (generously provided by G. Pazour, Worcester Foundation, Shrewsbury, MA) in the λDASHII vector (Stratagene) was screened using a DNA fragment from one clone obtained in the first screen as a hybridization probe. Plasmid pB1A10 (Figure 1) was constructed by digesting the λ clone 3A10 with *Xba*I, yielding an 11-kb fragment that was ligated into pBluescript (Stratagene). The pB1A10 plasmid was digested with *Pst*I to generate probe 3 (Figure 1) that was used to screen a cDNA library. The cDNA library was prepared in the λEXlox vector by Novagen, Inc. (Madison, WI) from poly(A)$^+$ RNA isolated from the wild-type strain A55 (Schnell and Lefebvre, 1993). The cDNA insert was excised from the λEXlox vector by digesting λ DNA with *Eco*RI and

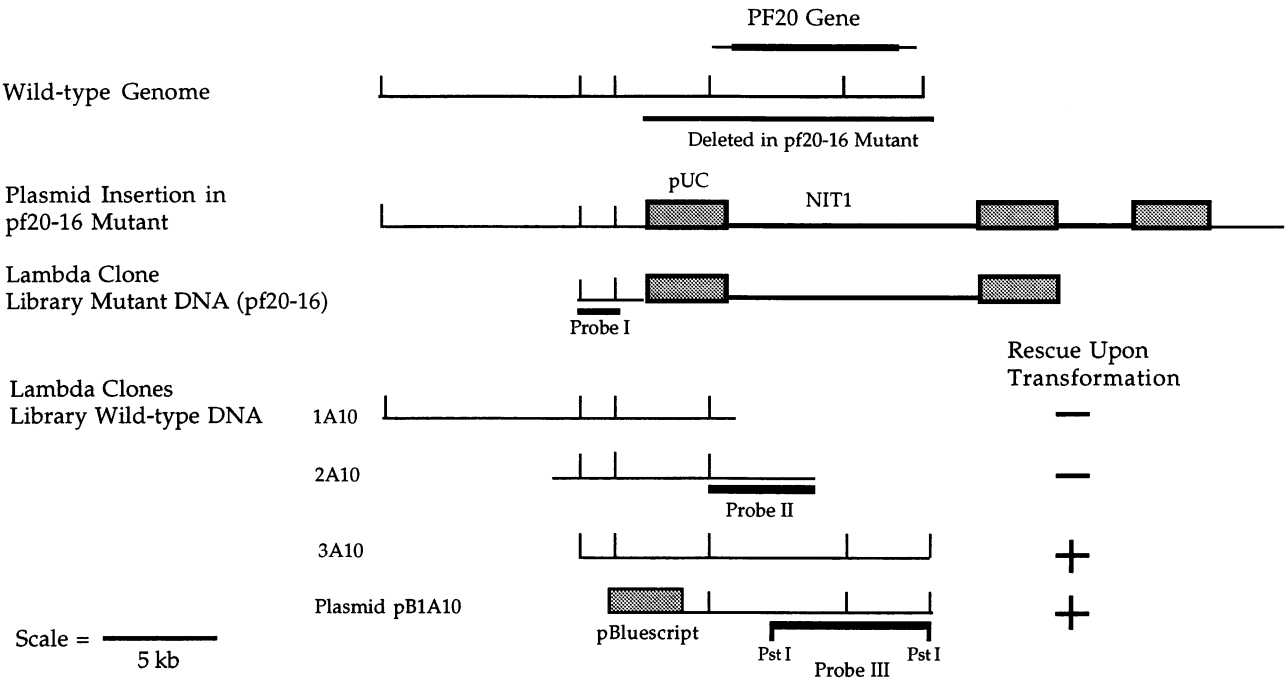

Figure 1. Restriction map of overlapping λ clones. Probe 1 is a 1.5-kb *Not*I fragment flanking the insertion site in the mutant strain *pf20–16* used to screen the wild-type genomic library to obtain clones 1A10 and 2A10. Probe 2 is a 4.8-kb *Not*I fragment used to screen the library a second time. Clone 3A10 was obtained in the second screen and rescued the paralyzed flagella phenotype when transformed into *pf20–16* mutant cells. The plasmid pB1A10 was constructed by digesting clone 3A10 with *Xba*I and ligating the indicated 11-kb fragment into the pBluescript vector. Probe 3 is a 7-kb *Pst*I fragment of pB1A10 used to screen a cDNA library and as a probe on RNA blots.

*Hin*dIII, and was ligated into the vector pUC119 for sequence analysis.

To determine whether λ clones rescued the motility defects in strain A10 or *pf20.3C*$^+$, cells were transformed with a cloned selectable marker gene and the λ clone being tested. For *pf20–16*, an *arg7*, *pf20-16* double mutant was constructed and transformed with the plasmid pARG7.8 (containing the arginino-succinate lyase gene; Debuchy *et al.*, 1989) and putative genomic clones for *PF20*. Transformants were selected as colonies growing on media without arginine supplement. In transformation experiments using *pf20.3C*$^+$ cells as host, emetine resistance was used as a dominant selectable marker. The cells were transformed with both a λ clone being tested and the plasmid pJN4 containing a mutant copy of the gene for ribosomal protein S14 which confers resistance to emetine upon transformation (Nelson *et al.*, 1994).

RNA Preparation, RNA Blots

Wild-type and mutant (strain A10 and *pf20.3C*$^+$) cells were grown in 250 ml of TAP media to mid to late log phase. The cells were divided into two aliquots, one of which was deflagellated by pH shock. Total RNA was prepared from nondeflagellated cells and from cells 45 min after deflagellation (Wilkerson *et al.*, 1994). Poly(A)$^+$ RNA was prepared by batchwise adsorption to oligo(dT)-Sepharose (Life Technologies, Gaithersburg, MD). Approximately 10 μg of poly(A)$^+$ RNA were fractionated on formaldehyde agarose gels (Sambrook *et al.*, 1982), then transferred to Hybond N$^+$ membranes (Amersham, Arlington Heights, IL), and hybridized with ^{32}P-labeled probe 3 (Figure 1) according to the manufacturer's instructions.

DNA Sequence Analysis

Both strands of the cloned cDNA were sequenced using Sequenase 2.0 (United States Biochemical Corp., Cleveland, OH) according to the manufacturer's instructions. For some templates, sequencing was performed by the DNA Sequencing Facility (Iowa State University, Ames, IA). The GCG programs were used for sequence assembly (Devereux *et al.*, 1984). Searches of the GenBank and SwissProt databases for sequence homologies were performed using the FASTA and BLAST programs (Altschul *et al.*, 1990).

Fusion Protein Expression and Antibody Production

The pEXlox vector containing the *PF20* cDNA was digested with *Sac*I and *Hin*dIII to release a 2.3-kb insert fragment that was then ligated into the pET30a vector (Novagen, Madison, WI) digested with *Sac*I and *Hin*dIII. The resulting fusion protein contains a 6x His tag at the amino terminal end. The pET30a-*PF20* construct was transformed into BL21(DE3) cells carrying the pLysS plasmid and plated on LB plates containing 30 μg/ml kanamycin. For induction of gene expression, cells were grown at 37°C to a density of OD_{600} (0.6–1), and fusion protein synthesis was induced by adding 1 mM isopropyl-thio-β-D-galactoside. After incubation for 2 h, the cells were suspended in 6 M urea, 5 mM imidizole, 0.5 M NaCl, and 0.02 M Tris-HCl (pH 8) and lysed by freezing at −80°C and thawing. Recombinant protein was purified from the resulting lysate by binding to Ni^2 NTA resin as recommended by the supplier (QIAGEN, Inc. Chatsworth, CA). Eluate fractions were analyzed by SDS-PAGE on 10% polyacrylamide gels stained with Coomassie blue. Peak fractions which contained pure fusion protein were pooled, and protein concentrations were determined using the Bradford reagent. Three injections of 100 μg of pure protein each were used to generate polyclonal antibodies in rabbits (Spring Valley Laboratories, Sykesville, MD). Sera collected after the second boost following primary injection showed high specificity for PF20 protein on immunoblots of flagellar proteins. For immunoblots, flagella were isolated as described (Smith and Lefebvre, 1996) and

75 μg of protein were loaded into each lane of a 10% polyacrylamide minigel. The proteins were transferred electrophoretically to a polyvinyldifluoridine difluoride membrane. For primary antibody incubations, the sera were diluted 1:10,000. Anti-*PF20* binding to immunoblots was detected with alkaline phosphatase conjugated to goat anti-rabbit IgG (Bio-Rad, Richmond, CA) and developed with 5-bromo-4-chloro-3-indolyphosphate/nitroblue tetrazolium (Harlow and Lane, 1988).

Immunolocalization

For immunolocalization experiments, the sera collected after the second boost following primary injection were affinity purified using the recombinant PF20 protein that had been electroblotted onto polyvinylidene difluoride membrane (Millipore, Bedford, MA). Binding and elution of the antibody was performed as described by Talian *et al.* (1983). For immunofluorescence experiments, flagella were isolated as described previously (Smith and Lefebvre, 1996). Fixation, permeabilization, and antibody incubation steps were carried out as described by Sanders and Salisbury (1995) using purified PF20 antibody as the primary antibody and goat anti-rabbit fluorescein isothiocyanate-conjugated secondary antibodies (Cappel, Organon Technika, Durham, NC) diluted 1:500. For immunogold labeling, flagella were isolated from A54-e18 cells, resuspended in HMDEK (10 mM HEPES, 5 mM $MgSO_4$, 1 mM dithiothreitol, 0.5 mM EGTA, 25 mM KCl), and allowed to settle onto formvar-coated, carbon-stabilized nickel grids. All subsequent antibody incubation steps were carried out as described in the study by Bernstein *et al.* (1994) using purified PF20 antibody as the primary antibody and 12 nm, gold-conjugated secondary antibodies (goat anti-rabbit, Jackson Immunologicals, Westgrove, PA) diluted 1:40. Control experiments in which the primary antibody was omitted were also performed. The central pair of microtubules were easily identified by eye, since their diameter is smaller than that of the doublet microtubules and the length and spacing of their associated projections is distinct from that of the radial spokes attached to the doublets.

RESULTS

Transformation and Mutant Screen

Mutants were generated by transforming *nit1* (nitrate reductase-deficient) cells with a plasmid containing the cloned *NIT1* gene (Fernandez *et al.*, 1989; Kindle *et al.*, 1989; Smith and Lefebvre, 1996). Colonies were picked into liquid media and visually screened for motility defects. Mutants with central apparatus defects characteristically have rigid flagella (Randall *et al.*, 1964; 1967). Axonemes were isolated from all cells with paralyzed flagella of wild-type length and were analyzed by electron microscopy. An analysis of axonemal cross-sections revealed that 95% of axonemes from the mutant strain A10 completely lacked central microtubules, a phenotype previously described for strains carrying the *pf15*, *pf18*, *pf19*, and *pf20* mutations (Randall *et al.*, 1964; 1967; Warr *et al.*, 1966).

Genetic Analysis

The A10 strain was backcrossed to a *nit1* mutant to determine whether the central apparatus defect cosegregated with the Nit^+ phenotype. Tetrad analysis revealed that the Nit^+ phenotype cosegregated with flagellar paralysis in at least 24 complete tetrads in each of two backcrosses, indicating that the lesion in the A10 strain was most likely caused by the integration of the transforming plasmid DNA. The mutation in the strain A10 was then tested for allelism with mutations known to produce defects in the central apparatus. In crosses of A10 cells with cells carrying the *pf15* (Witman *et al.*, 1978), *pf18*, and *pf19* (Adams *et al.*, 1981; provided by M. Porter, University of Minnesota) mutations, recombinant progeny were obtained. However, in crosses of strain A10 with the *pf20* mutant, no recombinants were obtained in 24 complete tetrads. Allelism was established by constructing stable diploids. Heterozygous diploids constructed by crossing A10 cells and *pf20* cells have paralyzed flagella, indicating that these mutations are allelic. There are 15 previously identified alleles of the *pf20* mutation (Adams *et al.*, 1981); therefore, the insertional allele was designated *pf20–16*.

Cloning the PF20 Gene

To begin cloning the *PF20* gene, a fragment of DNA flanking the site of plasmid integration was cloned from genomic DNA isolated from *pf20–16* cells. We determined that the *pf20–16* mutant contained several copies of the plasmid by hybridizing the pUC119 vector to genomic DNA on gel blots (see Figure 1 for map of insertion). Although genomic DNA analysis suggested that the *pf20–16* genome contained intact copies of the pUC119 vector, attempts to use a plasmid rescue technique to clone genomic fragments adjacent to the site of insertion were unsuccessful. Therefore, a library was constructed from *pf20–16* genomic DNA to clone DNA fragments flanking the insertion site. Phages containing genomic DNA adjacent to the site of plasmid insertion were identified using the 5′ end of the *NIT1* gene as a hybridization probe. This probe corresponds to a region of the *NIT1* gene deleted in the A54-e18 strain so that it will hybridize only to copies of the *NIT1* gene acquired upon transformation. λ DNA from plaques hybridizing to the probe was isolated and a restriction map was prepared. A 1.5-kb *Not*I fragment which contained only genomic sequence from *pf20–16* DNA and no plasmid sequence was identified (Figure 1). To confirm that the cloned sequence flanked the site of plasmid insertion, this 1.5-kb *Not*I fragment was used as a hybridization probe on blots of genomic DNA from *pf20–16* and wild-type (A54-e18) cells digested with a variety of enzymes (our unpublished observations). The probe hybridized to restriction fragments of different size on blots of DNA from *pf20–16* cells compared with that from wild-type cells, confirming that this probe represented DNA flanking the site of plasmid insertion in the mutant.

The 1.5-kb *Not*I probe (Figure 1, probe I) was then used to screen a bacteriophage λ library constructed from wild-type genomic DNA (Schnell and Lefebvre, 1993). Several overlapping clones were identified (Figure 1, clones 1A10 and 2A10) but none rescued the motility defect in *pf20–16* cells upon transformation. One possible explanation for failed rescue is that the complete wild-type copy of the gene was not contained in the clones tested. Insertion of exogenous DNA into *Chlamydomonas* frequently results in rearrangement and deletion of large portions of DNA (Tam and Lefebvre, 1993). Thus, if a sizable deletion occurred at the integration site, DNA clones flanking that site might be far from the *PF20* gene. Using labeled restriction fragments from clone 2A10 as probes on Southern blots of genomic DNA from *pf20–16*, a sizable deletion (greater than 15 kb) was detected. A 4.8-kb *Not*I fragment at the end of clone 2A10 extended into the region deleted in the mutant, and this fragment was used as a probe to rescreen the library (Figure 1, probe 2). No positive clones extending beyond the clone 2A10 were obtained. When the same probe was used to screen an unamplified λ library provided by Dr. G. Pazour (Worcester Foundation), a single clone, 3A10 (Figure 1), was obtained which extended beyond clone 2A10 into the region deleted in the mutant. This clone rescued the motility and ultrastructural defects in *pf20–16* and *pf20* cells upon transformation. The full extent of the deletion that occurred in *pf20–16* was not determined.

Rescue of pf20 Mutant Phenotypes by Transformation

To determine whether the λ clones obtained in our screen contained a functional *PF20* gene, we tested the ability of the λ clones to rescue the mutant phenotype in the insertional *pf20* allele, *pf20–16* and the previously identified *pf20* allele, *pf20.3C*$^+$. In these experiments the cells were cotransformed with a selectable marker gene and the λ clone being tested. For both mutants the transformants were picked into liquid media and screened for restoration of flagellar motility. To establish that rescue of the mutant phenotype correlated with incorporation of transforming DNA, genomic DNA was isolated from several transformed strains and analyzed by Southern blot hybridization. In all cases the rescued cells contained DNA from the transforming λ clone, indicating that the phenotypic rescue was most likely due to the function of the transgene. Ultrastructural analysis of axonemes isolated from rescued cells revealed that for both *pf20–16* and *pf20.3C*$^+$ strains the central apparatus was restored (Figure 2). Table 1 summarizes these results. In the rescued mutants, the number of central microtubules observed in axonemal cross-sections was comparable to the number of central microtubules observed in cross-sections of axonemes from wild-type cells.

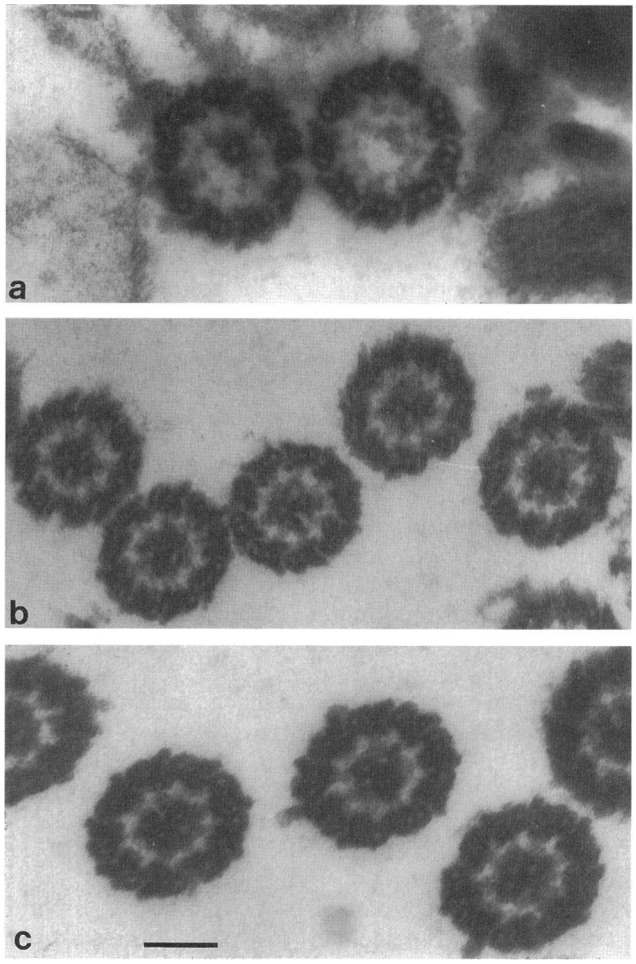

Figure 2. Thin section electron microscopy of axonemes from the mutant *pf20–16* (a) and from rescued mutants *pf20–16* (b) and *pf20.3C*$^+$ (c) transformed with the cloned *PF20* gene. Panels are representative axonemal cross-sections. Bar, 200 nm.

Table 1. Rescue of *pf20-16* and *pf20.3C*$^+$ by transformation

	No. of central tubules present (%)		
Mutant	0	1	2
Wild-type	6	12	81
pf20-16	73	27	0
pf20.3C$^+$ Transformant	9	0	91
pf20-16 Transformant	3	5	92

Percentiles represent at least 100 cross-sections of axonemes isolated from each strain.

Transcript Analysis and cDNA Sequence

To characterize the transcript of the *PF20* gene and to obtain the amino acid sequence of its predicted gene product, cDNA clones were isolated and sequenced. To prepare an appropriate hybridization probe for screening a cDNA library, the extent of the *PF20* gene was defined by subcloning λ clone 3A10 into smaller fragments and testing each subclone for the ability to rescue flagellar paralysis upon transformation. The smallest subclone that rescued the mutant phenotype was an 11-kb *Xba*I fragment subcloned into pBluescript (Figure 1, pB1A10). A *Pst*I fragment from clone pB1A10 (Figure 1, probe 3) was then used as a hybridization probe for RNA blots.

Poly(A)$^+$ RNA was prepared from *pf20–16*, *pf20.3C*$^+$, and wild-type cells before and 45 min after deflagellation. Deflagellation in *Chlamydomonas* causes increased accumulation of transcripts from genes encoding flagellar proteins (reviewed in Lefebvre and Rosenbaum, 1986). Hybridization of probe 3 (Figure 1) to blots of size-fractionated RNA revealed a 2.6-kb transcript that accumulated following deflagellation in wild-type cells (Figure 3, lanes 1 and 2). As expected, no detectable transcript was observed in RNA isolated from the mutant *pf20–16* (Figure 3, lanes 3 and 4) because the *PF20* gene is deleted in this mutant. A transcript of the expected size was present in RNA from *pf20.3C*$^+$ cells, although transcript levels were low relative to wild-type cells and the transcript did not accumulate following deflagellation.

A wild-type *Chlamydomonas* cDNA library prepared from poly(A)$^+$ RNA isolated from wild-type cells was screened using probe 3 (Figure 1). The largest clone obtained had a 2.6-kb insert. The DNA sequence of the 2.6-kb cDNA revealed a single, long open reading frame whose putative translation initiation codon is preceded by an upstream in-frame termination codon (Figure 4, double underline). Therefore, the 2.6-kb insert appeared to contain the complete coding sequence of the PF20 protein with an open reading frame encoding 606 amino acids.

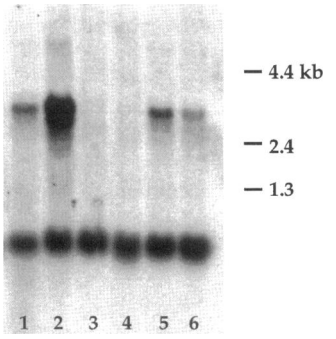

Figure 3. RNA blot. Ten micrograms of poly(A)$^+$ RNA prepared from cells before and 45 min after deflagellation were loaded in each lane. A radiolabeled 7-kb *Pst*I restriction fragment of plasmid pB1A10 (Figure 1, probe 3) was used as a hybridization probe. The *S14* gene (encoding the ribosomal S14 protein) is constituitively expressed and was used as a hybridization probe to control for equal loading. Lanes 1, 3, and 5 contain RNA from cells before deflagellation. Lanes 2, 4, and 6 contain RNA from cells 45 min after deflagellation. Lanes 1 and 2 contain RNA from wild-type cells, lanes 3 and 4 contain RNA from *pf*20–16 cells, and lanes 5 and 6 contain RNA from *pf20.3C*$^+$ cells. The band of 1 kb represents the transcript of the *S14* gene.

Analysis of the Predicted PF20 Gene Product

The predicted PF20 protein of 606 amino acids has an isoelectric point of 6.56 and mass of 65.8 kDa. The gene product contains five contiguous G-β repeats (Fong *et al.*, 1986) in the carboxyl-terminal half of the protein (Figure 4, underlined). Four of these repeats were identified using the MOTIFS program in the GCG suite of sequence analysis programs (Devereux *et al.*, 1984). The first G-β repeat was identified by eye and conforms well to the G-β consensus described by Neer *et al.* (1994) of $\{X_{6-94} - [GH\text{-}X_{23-41} - WD]\}^n$ except WD is replaced by WH. All five repeats conform to the more extensive consensus proposed by Neer *et al.* (1994; Figure 5). Within the PF20 protein, the spacing of amino acids within and between the five WD repeats is highly conserved. In each case there are 27 amino acids between GH and WD within a repeat and 11 amino acids between the WD of one repeat and the GH of the next repeat.

Database searches using only the amino half of the protein revealed no significant homology with any previously identified protein sequences. Structurally, this region appears to be largely coiled coil, containing three distinct regions including an acidic, a basic, and an alanine-rich region (Figure 6). In the region of amino acids 7–38, 50% are acidic; from amino acids 151–183, 44% are basic; and from amino acids 151–205, 37% are basic. Immediately upstream from the WD repeats there is an alanine-rich region. From amino acids 263–283, 45% are alanine residues; from amino acids 242–313, 31% are alanine residues.

In searches of the expressed sequence tag databases for *PF20* homologues, many sequences were identified that contained WD repeats but no similarities to *PF20* outside of the repeats. However, one human cDNA sequence was identified whose predicted protein sequence showed extensive similarity to *PF20* in a region near the amino terminus. The sequence of clone N51175 was 62% identical and 72% similar to *PF20* over a stretch of 47 amino acids (Figure 7). Only a very short stretch of sequence from the N51175 clone was available for comparison; therefore, we do not know whether this protein contains WD repeats. However, because of the high amino acid sequence identity and because no other homologues were found using the amino-terminal half of the PF20 protein in searches of other databases, it is likely that N51175 is a bona fide human homologue of *PF20*.

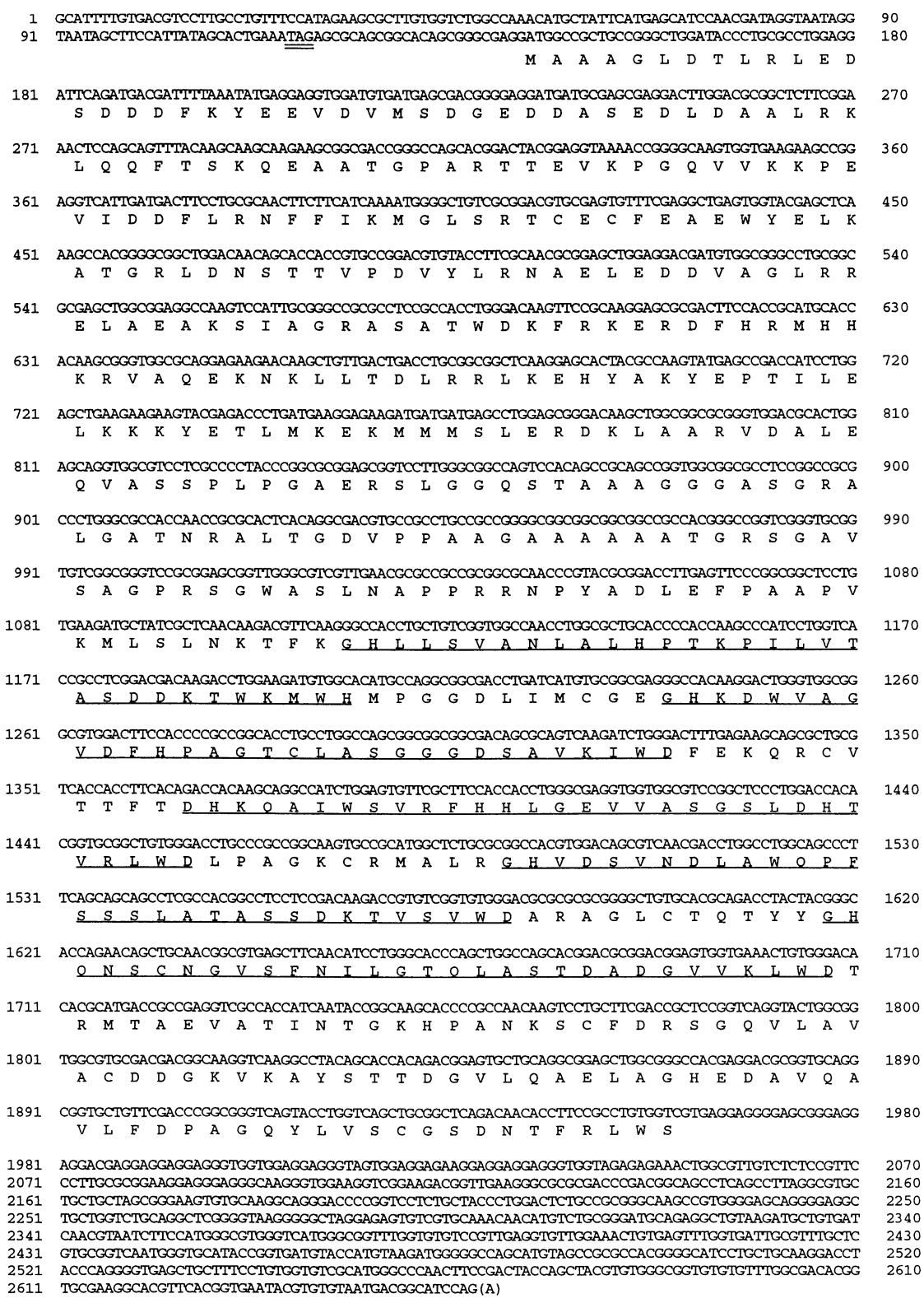

Figure 4. Sequence of *PF20* cDNA. The longest open reading frame predicted by the sequence is indicated. The region containing the five WD repeats is underlined. The in-frame stop codon upstream of the predicted initiation codon is indicated by double underlines. These sequence data are available from GenBank/EMBL/DDBJ under accession number U78547.

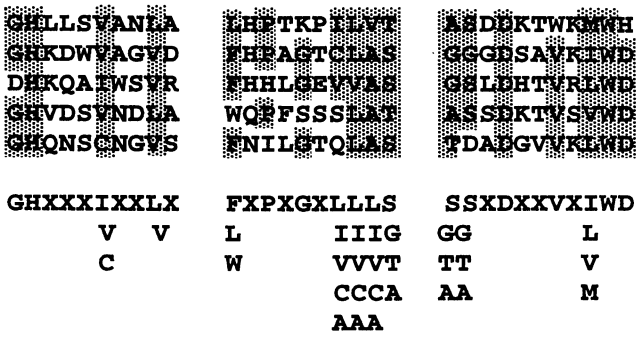

Figure 5. Alignment of the five WD repeats found in the predicted *PF20* gene product. The universal consensus of Neer *et al.* (1994) is presented below the alignment. Vertical rows conforming to the universal consensus of Neer *et al.* (1994) are highlighted.

Fusion Protein Expression and Purification, Antibody Production, and Localization

To localize the *PF20* gene product in axonemes, antibodies were generated to a fusion protein expressed in *Escherichia coli* cells. The expressed *PF20* construct lacked 101 amino acids from the amino terminus for a total of 505 amino acids and contained six additional histidine residues at its amino terminus, making it possible to purify the expressed fusion protein by binding to a nickel column. As assessed by SDS-PAGE, large quantities of pure fusion protein of the expected size (~50 kDa) were found in the eluate. Polyclonal antisera were prepared in rabbits using the purified protein as antigen.

The resulting sera were analyzed on protein blots of flagella prepared from five cell strains: wild-type (A54-e18), *pf20–16*, and *pf20.3C*$^+$ as well as *pf20–16* and *pf20.3C*$^+$ cells in which the mutant phenotype had been rescued by transformation with pB1A10. At a dilution of 1:10,000, the unpurified sera recognized a single protein of the expected size (~67 kDa) in flagella from wild-type and rescued cells (Figure 8, lanes 1, 3, 4, and 6) but no band was observed in flagella

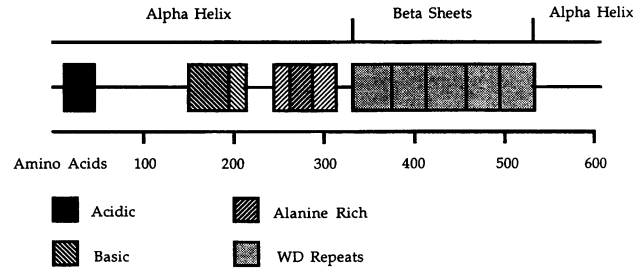

Figure 6. Gene structure. The amino-terminal half of the PF20 protein is comprised of an acidic (■), a basic (▧), and an alanine-rich region (▨). The carboxyl terminus is largely comprised of WD repeats (▩). Possible extensions of the basic and alanine-rich regions are more lightly shaded.

```
PF20          PEVIDDFLRN FFIKMGLSRT CECFEAEWYE LKATGRLDNS TTVPDVY
              ||||+||| | | ||||++|| ||++|||| ||    |      |||||
EST N51177    PEVIEDFLCN FLIKMGMTRT LDCFQSEWYE LKGVTELRTV GNVPDVY
```

Figure 7. Comparison of *PF20* cDNA sequence to EST clone N51175. Solid lines indicate identity and + indicates conserved substitutions.

from the mutant strains *pf20–16* or *pf20.3C*$^+$ (Figure 8, lanes 2 and 5). These results indicate that the antibody is specific for the PF20 protein.

For immunolocalization experiments, affinity-purified antibodies were obtained using the expressed PF20 fusion protein. In immunofluorescence experiments using whole-mount preparations of flagella from wild-type and mutant cells, staining was observed along the length of wild-type flagella whereas no staining was observed in flagella from *pf20.3C*$^+$ cells (our unpublished observations). We did not assay for the presence of the PF20 protein in the cell bodies. To localize the *PF20* gene product more precisely, immunogold electron microscopy was performed. Whole mounts of flagella from wild-type cells were prepared for immunogold labeling and negatively stained for electron microscopy. The three types of images most commonly found are presented in Figure 9. The most extensive decoration of flagella by gold particles was observed in preparations in which one of the central microtubules had disintegrated (Figure 9a). In these cases, a long line of gold particles was observed, probably indicating the previous position of the disintegrated microtubule. Since the remaining singlet microtubule had relatively long projections characteristic of the C1 microtubule, the disintegrated microtubule is most likely C2. The second type of staining was observed in preparations in which the two microtubules of the central apparatus had splayed apart (Figure 9b). In this case gold particles were always found associated with only one microtubule; based on the presence of short projections on the gold-labeled microtubule, this microtubule is most likely C2. The third type of staining was observed in preparations in which the central apparatus was largely intact but had short regions in which the two microtubules had separated. In these cases gold particles were only observed between the two microtu-

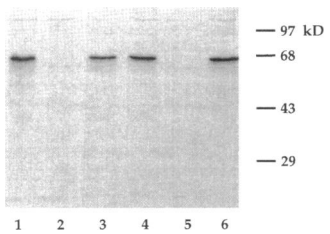

Figure 8. Immunoblot of flagellar protein. Approximately 75 μg of protein from isolated flagella were loaded into each lane. The purified PF20 antibody recognizes a protein of the expected size (67 kDa) present in flagella of wild-type cells (lanes 1 and 4), rescued *pf20–16* cells (lane 3), and rescued *pf20* cells (lane 6). No band is seen in flagella of the mutant *pf20–16* (lane 2) or *pf20* (lane 5).

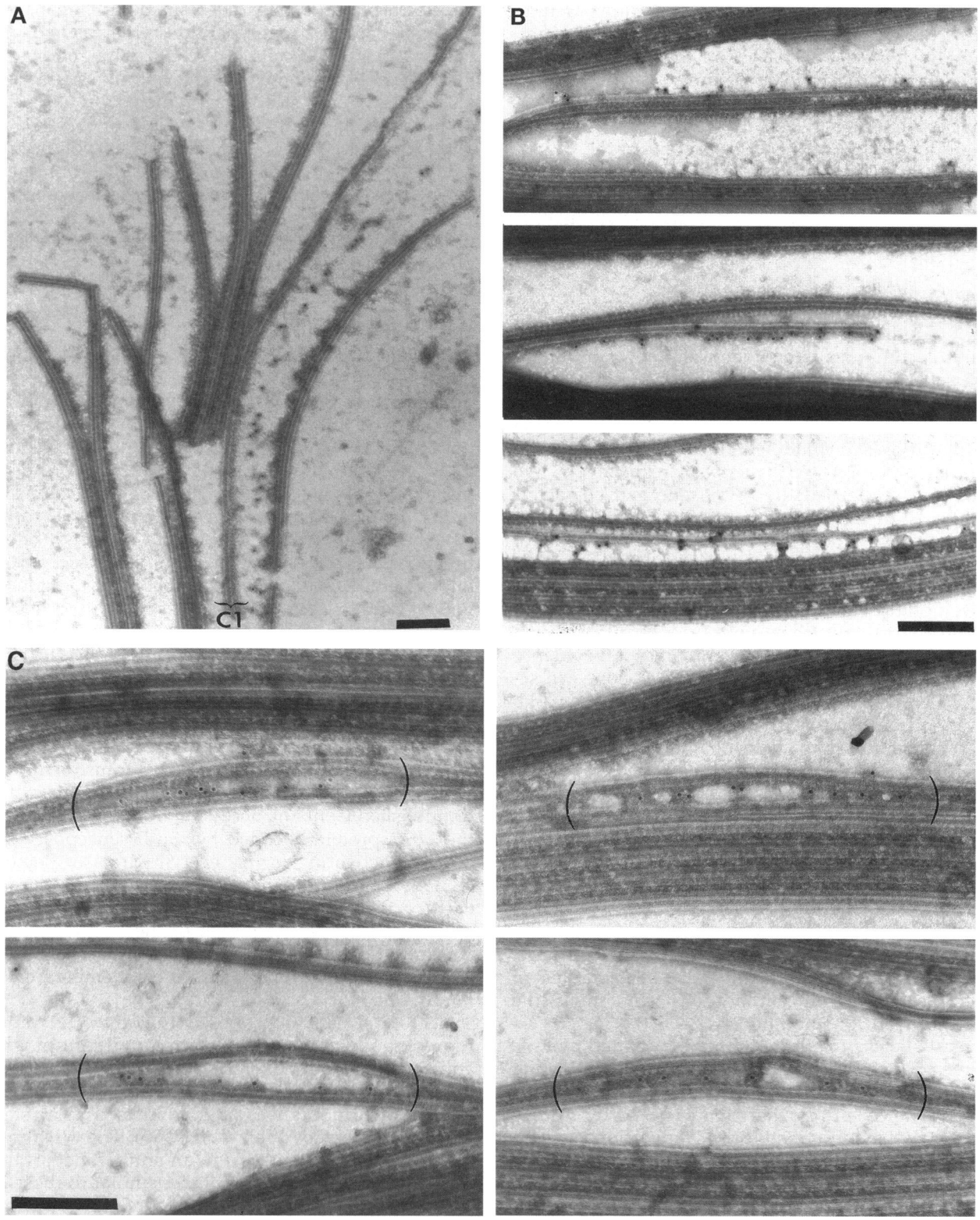

Figure 9. Localization of the *PF20* gene product in flagella by immunogold labeling. In A, the C1 microtubule of the central apparatus is intact (labeled C1) but the C2 tubule has disintegrated with only a line of gold particles remaining. In B, the two central tubules have splayed apart and gold labeling is only observed on the microtubule with the shortest projections (C2). In C, the central microtubules are still attached to each other except in short regions (parentheses) where gold particles localize to the central microtubule bridges. Bar, 200 nm.

bules in the region of separation and appeared to localize to structures connecting the two central microtubules (Figure 9c). Based on these observations, we conclude that the PF20 protein is primarily bound to the C2 microtubule and is associated with the connecting structure between the two central microtubules. The binding of the PF20 protein to the C2 microtubule may be direct or may involve additional polypeptides specifically bound to C2. No gold particles were observed bound to axonemes when incubation with the primary antibody was omitted.

DISCUSSION

We have undertaken a molecular dissection of central apparatus components by generating new central apparatus defective mutants using an insertional mutagenesis technique. In our initial mutant screen, we identified several central apparatus mutants including D2 and A10 which contained alleles of the previously identified mutations *pf16* and *pf20*, respectively. We cloned and sequenced the *PF16* gene and characterized the *PF16* gene product (Smith and Lefebvre, 1996). Here, we report the cloning and sequencing of the *PF20* gene and localization of the *PF20* gene product.

Although the smallest genomic clone that could rescue the *pf20* mutant phenotype upon transformation was quite long (~11 kb), several lines of evidence support the conclusion that the cDNA clone we sequenced corresponds to the *PF20* transcript. The 7-kb restriction fragment used to screen the cDNA library represents more than half of the genomic clone pB1A10. Transformation using this clone rescued the *pf20* mutant phenotype. The labeled 7-kb restriction fragment hybridized to a single transcript on blots of RNA isolated from wild-type cells. This transcript was missing from RNA prepared from cells containing the deletion mutation, *pf20–16*. The transcript was reduced in abundance from RNA prepared from cells containing the previously described allele, *pf20.3C*$^+$. Finally, antibodies generated against the gene product of the cDNA we obtained do not detect antigen in flagella isolated from either cells containing the *pf20–16* or *pf20.3C*$^+$ mutations.

Several alleles of *pf20* were initially isolated by R.A. Lewin and first characterized structurally by Randall *et al.* (1964). Additional alleles of *pf20* were subsequently isolated and further characterized by Adams *et al.* (1981); they described the *pf20* mutation as being "leaky" in that a small percentage of the cells in the population were swimming, and reported that 35% of flagellar cross-sections contained two central microtubules, apparently wild type in ultrastructure. Upon demembranation to produce axonemes, however, 95% of the cross-sections showed the loss of the entire central apparatus. In addition, using two-dimensional gel electrophoresis, they determined that flagella from *pf20* cells lacked six polypeptides whereas axonemes isolated from *pf20* cells lacked 18 polypeptides they identified as components of the central apparatus.

The *PF20* gene encodes a predicted protein of 606 amino acids with a molecular weight of 65.8 kDa and an isoelectric point of 6.56. Of the six polypeptides Adams *et al.* (1981) detected as missing from flagella isolated from *pf20* cells, one of these polypeptides, CP13, has a molecular weight (62 kDa) similar to that of the predicted PF20 protein. However, the isoelectric point of CP13 is very different (about 8) from that predicted for the *PF20* gene product. Therefore, the *PF20* gene product probably does not correspond to CP13 and may not have been identified in previous biochemical analyses of central apparatus components.

Database searches using the predicted amino acid sequence of PF20 placed the protein in a family of proteins which contain repeat domains first identified in the β-subunit of the heterotrimeric GTP-binding protein β-transducin (Fong *et al.*, 1984) and named G-β or WD repeats. Many proteins containing WD repeats have been identified and perform a variety of cellular functions. Neer *et al.* (1994) grouped these proteins into several functional classes including proteins involved with signal transduction, RNA processing, gene regulation, vesicular traffic, and regulation of cytoskeletal assembly. More recently, the WD repeat motif has also been identified in the IC69 and IC78 intermediate chains of outer arm flagellar dyneins of *Chlamydomonas* (Wilkerson *et al.*, 1995). In homology searches using the predicted PF20 amino acid sequence, the first three matches are β-transducin (Fong *et al.*, 1986), a protein kinase (*Thermomonospora curvata*; unpublished GenBank accession number U23820) and the LIS-1 protein encoded by the lissencephaly gene (platelet activating factor, acetylhydrolase; Reiner *et al.*, 1993). Because alignment of the PF20 protein with each of these protein sequences revealed significant homology only in the region of the WD repeats, we conclude that *PF20* is not the *Chlamydomonas* homologue of any previously identified members of this family.

Neer *et al.* (1994) proposed that the WD repeats represent a highly conserved structural unit in which anti-parallel β-strands form a conserved core with variable regions displayed on the surface. The structure of such motifs was later confirmed in crystallographic analyses by Wall *et al.* (1995). The WD repeats contain multiple β-strands in an antiparallel arrangement. Four β-strands form blades similar to those of a propeller in which the conserved core of the WD motif forms three inner β-strands of one blade and the variable amino-terminal portion of each repeat contributes to the fourth outer strand of each blade. In this arrangement, the conserved core is viewed as a scaffold

to display the variable regions between repeats. The diversity of function for proteins containing these repeats may be explained by the number and spacing of the repeats as well as the variable region sequence. For all WD repeat containing proteins, however, these structures allow for specific interactions with other proteins to form protein complexes. Given the *pf20* mutant phenotype, most likely the PF20 protein forms a complex with additional polypeptides, and this complex is required for assembly or stability of the central pair microtubules.

In addition to the WD repeats, the PF20 protein also contains distinct regions rich in basic and acidic amino acids as well as an alanine-rich region. The PF20 protein does not encode a known microtubule-binding domain such as those identified in microtubule-associated proteins from neurons. The only microtubule-binding domains described for flagellar proteins to date are for a component of the radial spokes (RSP3) and a dynein intermediate chain (IC78). Using in vitro reconstitution approaches, Diener *et al.* (1993) identified an 85-amino acid region of RSP3 which is required for binding to the doublet microtubules of axonemes. This region is very basic in amino acid composition, but shares no homology with known microtubule-binding motifs or with the *PF16* or *PF20* gene products. King *et al.* (1995) reported that basic regions within the IC78 intermediate chain of flagellar outer dynein arms may form microtubule-binding domains. IC78 deletion constructs lacking these basic domains no longer bound to microtubules or axonemes in reconstitution assays. Whether the basic region in the PF20 protein also has a microtubule-binding function will require similar analyses. We do not know the significance of the alanine-rich region. Because this alanine-rich region separates the WD repeats from the amino-terminal half of the PF20 protein, it may serve as a linker element between the WD repeats and this region.

With polyclonal antibodies generated using the expressed *PF20* cDNA as an antigen, the *PF20* gene product was localized along the length of the C2 central microtubule. *PF20* may bind directly to the C2 microtubule or may bind to other polypeptides which are specifically bound to the C2 tubule. The PF20 protein appears to localize to the intermicrotubule links connecting C1 and C2 and not to the C2 projections. This conclusion is supported by our observation that when the central apparatus is intact, gold labeling is only observed in regions where the C1 and C2 tubules are partially separated. The best gold labeling observed is when the two microtubules have completely splayed apart, exposing the antigen, or the microtubule lattice of C2 has disintegrated altogether, allowing complete antigen accessibility.

Previously, we reported that *PF16* localizes to the projections of the C1 microtubule (Smith and Lefebvre, 1996). Bernstein *et al.* (1994) reported that KLP-1 localizes to the projections of the C2 microtubule, and Miller *et al.* (1990) reported that a protein similar to a kinetochore antigen localizes to the tips of ciliary microtubules. The results we describe here represent the first report of localization of a specific polypeptide to the cross-linking structures of the two central microtubules in flagellar axonemes. Warner (1976) and Linck *et al.* (1981) have described central microtubule bridges for both mussel gill cilia and squid sperm, respectively, as having an axial repeat of 16 nm. Interestingly, using optical diffraction techniques to study central apparatus ultrastructure, Linck *et al.* (1981) observed that the central tubule bridges are in exact register with structures on the surface of the C2 tubule and have a similar beaded appearance, indicating that the bridges may originate from the C2 tubule. This observation agrees with our finding that *PF20* is primarily associated with the C2 tubule but does not rule out the possibility that similar structures originate from the C1 tubule. Because axonemes from *pf20* cells are missing the entire central apparatus, the *PF20* gene product is most likely involved in forming these bridges and stabilizing the two microtubules of the central pair. Based on the gene sequence, localization, and mutant phenotype, one hypothesis is that the PF20 protein may bind to the C2 microtubule by its amino-terminal half, possibly through its basic region, and interact with other polypeptides via the WD repeat regions to form a stable intermicrotubule bridge. Candidates for such interacting polypeptides may include some of those reported as missing from *pf20* axonemes by Adams *et al.* (1981). The antibodies described in this report will be useful in cross-linking and immunoprecipitation experiments to determine which polypeptides interact with the *PF20* gene product and comprise these microtubule-cross-bridging structures.

ACKNOWLEDGMENTS

We thank Mark Sanders of the Imaging Center, College of Biological Sciences, University of Minnesota for technical assistance in figure production. We also thank B. Dentler and C. Silflow for useful comments on the manuscript. This work was supported by United States Public Health Service grant GM51379 to P.A.L.. E.F.S. was supported in part by NSF-RTG grant DIR-9113444 and ACS grant PF-3955.

REFERENCES

Adams, G.M.W., Huang, B., Piperno, G., and Luck, D.J.L. (1981). Central-pair microtubular complex of *Chlamydomonas* flagella: polypeptide composition as revealed by analysis of mutants. J. Cell Biol. *91*, 69–76.

Allen, C., and Borisy, G. (1974). Structural polarity and directional growth of microtubules of *Chlamydomonas* flagella. J. Mol. Biol. *90*, 381–402.

Altschul, S.F., Gish, W., Miller, W., Meyers, E.W., and Lipman, D.J. (1990). Basic alignment search tool. J. Mol. Biol. *215*, 403–410.

Bernstein, M., Beech, P.L., Katz, S.G., and Rosenbaum, J.L. (1994). A new kinesin-like protein (Klp1) localized to a single microtubule of the *Chlamydomonas* flagellum. J. Cell Biol. *125*, 1313–1326.

Binder, L., Dentler, W., and Rosenbaum, J. (1975). Assembly of chick brain tubulin onto flagellar axonemes of *Chlamydomonas* and sea urchin sperm. Proc. Natl. Acad. Sci. USA *72*, 1122–1126.

Chisholm, D. (1989). A convenient procedure for obtaining DNA from bacteriophage lambda. Biotechniques *7*, 21–23.

Curry, A.M., and Rosenbaum, J.L. (1993). Flagellar radial spoke: a model molecular genetic system for studying organelle assembly. Cell Motil. Cytoskeleton *24*, 224–232.

Debuchy, R., Purton, S., and Rochaix, J.D. (1989). The argininosuccinate lyase gene of *Chlamydomonas reinhardtii*: an important tool for nuclear transformation and for correlating the genetic and molecular maps of the *ARG7* locus. EMBO J. *8*, 2803–2809.

Dentler, W.L., and LeCluyse, E.L. (1982). The effects of structures attached to the tips of tracheal ciliary microtubules on the nucleation of microtubule assembly in vitro. Cell Motil. Suppl. *1*, 13–18.

Dentler, W.L., and Rosenbaum, J.L. (1977). Flagellar elongation and shortening in *Chlamydomonas*. III. Structural attachment to the tips of flagellar microtubules and their relationship to direction of microtubule assembly. J. Cell Biol. *74*, 747–755.

Devereux, Haeberli, J.P., and Smithies, O. (1984). A comprehensive set of sequence analysis programs for the VAX. Nucleic Acids Res. *12*, 387–395.

Diener, D.R., Ang, L.H., and Rosenbaum, J.L. (1993). Assembly of flagellar radial spoke proteins in *Chlamydomonas*: identification of the axoneme binding domain of radial spoke protein 3. J. Cell Biol. *123*, 183–190.

Dutcher, S.K. (1995). Flagellar assembly in two hundred and fifty easy-to-follow steps. Trends Genet. *11*, 398–404.

Dutcher, S.K., Huang, B., and Luck, D.J.L. (1984). Genetic dissection of the central pair microtubules of the flagella of *Chlamydomonas reinhardtii*. J. Cell Biol. *98*, 229–236.

Euteneuer, U., and McIntosh, JJ.R.. (1981). Polarity of some motility related microtubules. Proc. Natl. Acad. Sci. USA *78*, 372–376.

Fernández, E., Schnell, R., Ranum, L.P.W., Hussey, S.C., Silflow, C.D., and Lefebvre, P.A. (1989). Isolation and characterization of the nitrate reductase structural gene of *Chlamydomonas reinhardtii*. Proc. Natl. Acad. Sci. USA *86*, 6449–6453.

Fong, H.K.W., Hurley, J.B., Hopkings, R.S., Miake-Lye, R., Johnson, M.S., Doolittle, R.F., and Simon, M.I. (1986). Repetitive segmental structure of the transducin β subunit: homology to the CDC4 gene and identification of related mRNAs. Proc. Natl. Acad. Sci. USA *83*, 2162–2166.

Fox, L.A., Sawin, K.E., and Sale, W.S. (1994). Kinesin-related proteins in eukaryotic flagella. J. Cell Sci. *6*, 1545–1550.

Gorman, D.S., and Levine, R.P. (1965). Cytochrome f and plastocyanin: their sequence in the photosynthetic electron transport chain of *Chlamydomonas reinhardtii*. Proc. Natl. Acad. Sci. USA *54*, 1665–1669.

Harlow, E., and Lane, D. (1988). Antibodies: A Laboratory Manual, Cold Spring Harbor, NY: Cold Spring Harbor Laboratory Press.

Harris, E. (1989). The *Chlamydomonas* Sourcebook, San Diego, CA: Academic Press.

Hosokawa, Y., and Miki-Noumura, T. (1987). Bending motion of *Chlamydomonas* axonemes after extrusion of the central pair. J. Cell Biol. *105*, 1297–1301.

Howard, D.R., Habermacher, G., Glass, D., Smith, E.F., and Sale, W.S. (1994). Regulation of *Chlamydomonas* flagellar dynein by an axonemal protein kinase. J. Cell Biol. *127*, 1683–1692.

Johnson, K.A., Haas, M.A., and Rosenbaum, J.L. (1994). Localization of a kinesin-related protein to the central apparatus of the *Chlamydomonas reinhardtii* flagellum. J. Cell Sci. *6*, 1551–1556.

Kindle, K.L. (1990). High frequency nuclear transformation of *Chlamydomonas reinhardtii*. Proc. Natl. Acad. Sci. USA *87*, 1228–1232.

Kindle, K.L., Schnell, R.A., Fernández, E., and Lefebvre, P.A. (1989). Stable nuclear transformation of *Chlamydomonas* using a gene for nitrate reductase. J. Cell Biol. *109*, 2589–2601.

King, S.M., Patel-King, R.S., Wilkerson, C.G., and Witman, G.B. (1995). The 78,000-Mr intermediate chain of *Chlamydomonas* outer arm dynein is a microtubule-binding protein. J. Cell Biol. *131*, 399–409.

Lefebvre, P.A., and Rosenbaum, J.L. (1986). Regulation and assembly of ciliary and flagellar proteins during regeneration. Annu. Rev. Cell Biol. *2*, 517–546.

Linck, R.W., Olson, G.E., and Langevin, G. (1981). Arrangement of tubulin subunits in microtubule-associated proteins in the central pair microtubule apparatus of squid (*Loligo pealei*) sperm flagella. J. Cell Biol. *89*, 309–322.

Lux, F.G., II, and Dutcher, S.K. (1991). Genetic interactions of the *fla10* locus: suppressors and synthetic phenotypes that affect the cell cycle and flagellar function in *Chlamydomonas reinhardtii*. Genetics *128*, 549–561.

Miller, J.M., Wang, W., Balczon, R., and Dentler, W.L. (1990). Ciliary microtubules contain a mammalian kinetochore antigen. J. Cell Biol. *110*, 703–714.

Neer, E.J., Schmidt, C.J., Nambudripad, R., and Smith, T.F. (1994). The ancient regulatory-protein family of WD-repeat proteins. Nature *371*, 297–300.

Nelson, J.A.E., Savereide, P.B., and Lefebvre, P.A. (1994). The *CRY1* gene in *Chlamydomonas reinhardtii*: structure and use as a dominant selectable marker for nuclear transformation. Mol. Cell. Biol. *14*, 4011–4019.

Omoto, C., and Kung, C. (1979). The pair of central tubules rotates during ciliary beat in *Paramecium*. Nature *279*, 532–534.

Piperno, G., Mead, K., and Shestak, W. (1992). The inner dynein arms I2 interact with a "dynein regulatory complex" in *Chlamydomonas* flagella. J. Cell Biol. *118*, 1455–1464.

Porter, M.E. (1996). Axonemal dyneins; assembly, organization and regulation. Curr. Opin. Cell Biol. *8*, 10–17.

Randall, J.T., Warr, J.R., Hopkins, J.M., and McVittie, A. (1964). A single gene mutation of *Chlamydomonas reinhardtii* affecting motility: a genetic and electron microscope study. Nature *203*, 912–914.

Randall, J.T., Cavalier-Smith, T., McVittie, A., Warr, J.T., and Hopkins, J.M. (1967). Developmental and control processes in the basal bodies and flagella of *Chlamydomonas reinhardtii*. Dev. Biol. Suppl. *1*, 43–83.

Reiner, O., Carozzo, R., Shen, Y., Wehnert, M., Faustinella, F., Dobyns, W., Caskey, C.T., and Ledbetter, D.H. (1993). Isolation of Miller-Dieker lissencephaly gene containing G protein β-subunit-like repeats. Nature *364*, 717–721.

Sager, R., and Granick, S. (1953). Nutritional studies in *Chlamydomonas reinhardtii*. Ann. NY Acad. Sci. *56*, 831–838.

Sambrook, J., Fritsch, E.F., and Maniatis, T. (1982). Molecular Cloning: A Laboratory Manual, Cold Spring Harbor, NY: Cold Spring Harbor Laboratory Press.

Sanders, M.A., and Salisbury, J.L. (1995). Immunofluorescence microscopy of cilia and flagella. In: Cilia and Flagella: Methods in Cell

Biology, vol. 47, ed. W. Dentler and G. Witman, New York: Academic Press, 163–169.

Schnell, R.A., and Lefebvre, P.A. (1993). Isolation of the *Chlamydomonas* regulatory gene *NIT2* by transposon tagging. Genetics *134*, 737–747.

Smith, E.F., and Lefebvre, P.A. (1996). *PF16* encodes a protein with armadillo repeats and localizes to a single microtubule of the central apparatus in *Chlamydomonas* flagella. J. Cell Biol. *132*, 359–370.

Smith, E.F., and Sale, W.S. (1992). Regulation of dynein-driven microtubule sliding by the radial spokes in flagella. Science *257*, 1557–1559.

Smith, E.F., and Sale, W.S. (1994). Mechanisms of flagellar movement: functional interactions between dynein arms and the radial spoke-central apparatus complex. In: Microtubules, ed. J. Hyams and C. Lloyd, New York: Wiley-Liss, Inc., 381–392.

Talian, J.C., Olmsted, J.B., and Goldman, R.D. (1983). A rapid procedure for preparing fluorescently labeled specific antibody from whole serum: its use in analyzing cytoskeleton architecture. J. Cell Biol. *97*, 1277–1282.

Tam, L.-W., and Lefebvre, P.A. (1993). Cloning of flagellar genes in *Chlamydomonas reinhardtii* by DNA insertional mutagenesis. Genetics *135*, 375–384.

Wall, M.A., Coleman, D.E., Lee, E., Inguez-Lluhl, J.A., Posner, B.A., Gilman, A.G., and Sprang, S.R. (1995). The structure of G protein heterotrimer $G_{i\alpha1\beta,\gamma2}$. Cell *83*, 1047–1058.

Warner, F.D. (1976). Ciliary inter-microtubule bridges. J. Cell Sci. *20*, 101–114.

Warner, F.D., and Satir, P. (1974). The structural basis of ciliary bend formation. Radial spoke positional changes accompanying microtubule sliding. J. Cell Biol. *63*, 35–63.

Warr, J.R., McVittie, A., Randall, J.T., and Hopkins, J.M. (1966). Genetic control of flagellar structure in *Chlamydomonas reinhardtii*. Genet. Res. *7*, 335–351.

Wilkerson, C.G., King, S.M., Koutoulis, A., and Pazour, G.J. (1995). The 78,000 Mr intermediate chain of *Chlamydomonas* outer arm dynein is a WD-repeat protein required for arm assembly. J. Cell Biol. *129*, 169–178.

Wilkerson, C.G., King, S.M., and Witman, G.B. (1994). Molecular analysis of the γ-heavy chain of *Chlamydomonas* flagellar outer arm dynein. J. Cell Sci. *107*, 497–506.

Witman, G.B. (1989). Perspective: composition and molecular organization of the dyneins. In: Cell Movement, vol. 1, ed. F.D. Warner, P. Satir, and I.R. Gibbons, New York: Alan R. Liss.

Witman, G.B., Plummer, J., and Sander, G. (1978). *Chlamydomonas* flagellar mutants lacking radial spokes and central tubules. Structure, composition, and function of specific axoneme components. J. Cell Biol. *76*, 729–747.